A nearly exact seismic modeling algorithm for frequency domain FWI

Wenyi Hu, Advanced Geophysical Technology Inc.*

Summary

To substantially accelerate frequency domain full waveform inversion, we developed an efficient and nearly exact seismic wave propagation modeling algorithm. The modeling engine is based on a finite-different time domain method but the output data is in frequency domain. In this algorithm, a 4-point stencil scheme (same computational cost as the 4^{th} order conventional finite difference method) is used while the accuracy is higher than the conventional 16^{th} order finite difference scheme. Furthermore, the accuracy level of this algorithm is independent of time step size due to two special techniques employed: 1) dispersion minimization algorithm (a nonlinear inversion algorithm) incorporating both spatial and temporal discretization and propagation angle; 2) optimized time integration based on finite impulse response (FIR) filter design technology. This algorithm does not suffer from artificial anisotropy, which can be a serious issue in the conventional finite difference method when the grid size is relatively large or the grid sizes are different in lateral and vertical directions. This method is applicable to 2D, 3D, anisotropic, and elastic cases. Numerical examples are presented to show its performance is actually better than the conventional 16^{th} order finite difference with much lower computational expense.

Introduction

Recent years, many research efforts have been made to improve the efficiency of full waveform inversion (FWI). Full waveform inversion is a power tool for reconstruction of complex geology structures and geophysical properties. Because it utilizes the full waveform information contained in recorded seismic data, FWI is able to provide high resolution velocity model and other geophysical property models such as anisotropic parameters, attenuation, density, and etc. FWI can be classified in two categories. The first category is the time domain FWI (Tarantola, 1986; Bunks et al, 1995; Vigh et al., 2010); the second is the frequency domain FWI (Pratt et al., 1998; Sirgue and Pratt, 2004; Plessix 2009). These two categories of FWI methods both have advantages and disadvantages (Vigh and Starr, 2008). Frequency domain FWI uses only several discrete frequencies; therefore the data redundancy is greatly reduced and the data volume is more compact to save memory use. In addition, frequency domain FWI is essentially a multi-scale method, which is better for nonlinearity mitigation.

Unfortunately, one of the bottle necks of frequency domain FWI methods is the efficiency of frequency domain forward modeling solver. Since the computational complexity increases geometrically with the size of model, frequency domain forward modeling direct solvers are impractical for large 3D problems. An alternative choice is the frequency domain iterative solver, whose efficiency is comparable with time domain solver, provided that a good preconditioner is applied. However, designing a good preconditioner is not trivial.

For this reason, we developed a highly efficient and accurate hybrid domain seismic wave propagation modeling algorithm, where a harmonic source (single frequency) is propagated in time domain, and the recorded time domain wavefields are gradually converted to frequency domain data during simulation. Most existing time domain methods and hybrid domain methods are based on the conventional finite difference scheme whose numerical dispersion is inevitable and can lead to huge phase error, eventually affecting the accuracy of velocity reconstruction in FWI algorithm. Higher-order (16^{th} or higher) finite difference scheme is accurate for smooth velocity model but it is computationally expensive. Moreover, it loses advantages where velocity model varies abruptly. Therefore, shorter stencil is preferred for cost saving and also for ease of parallelization. Some optimized finite difference methods suppress dispersion error to some extent. However, most of these methods assume a small Courant number or use high-order temporal finite difference scheme.

Our algorithm differentiates from other finite difference modeling algorithms in the following aspects: 1) with the fact that we only need to accurately compute one or several discrete frequency components, we design the update equation coefficients to specifically reduce the dispersion error and numerical anisotropy at these targeted frequencies; consequently, our algorithm has higher accuracy level compared with other optimized finite difference methods because it is usually not easy to suppress dispersion error substantially for wide-band data; 2) accuracy is independent of time step size because the time step size effect is taken into account in the coefficient design procedure, which is a nonlinear inversion process; 3) the time integration error during time-to-frequency domain conversion due to temporal discretization is reduced significantly through finite impulse response filter design technique.

Governing Equations and Conventional FDTD

Without losing generality, we use acoustic wave propagation equation as follows:

Nearly exact modeling algorithm for frequency domain FWI

$$\nabla p + j\omega\rho\mathbf{v} = \mathbf{f}$$
$$\nabla \cdot \mathbf{v} + j\omega\kappa p = q \quad (1)$$

where p is the pressure, $\mathbf{v}$ is the particle velocity, ρ is the mass density, $\mathbf{f}$ is the volume density of the body force, q is the volume density of mass, and κ is the compressibility.

The first step to numerically solve equation (1) is to discretize the equation with finite difference approximation. The conventional finite difference method (4^{th} spatial order and 2^{nd} temporal order) has the following scheme based on Taylor expansion:

$$\frac{\partial f_i}{\partial x} \approx \frac{\frac{9}{8}(f_{i+1/2} - f_{i-1/2}) - \frac{1}{24}(f_{i+3/2} - f_{i-3/2})}{\Delta x} \quad (2)$$

$$\frac{\partial f^n}{\partial t} \approx \frac{f^{n+1/2} - f^{n-1/2}}{\Delta t} \quad (3)$$

With this scheme, if Δt=2 ms, Δx=20 Hz, v_p= 1500 m/s, dispersion analysis shows that the numerical velocity is 1451 m/s. This level of dispersion error is unacceptable.

The New Finite Difference Scheme

To eliminate the above dispersion error, we developed an optimized new finite difference scheme (ONS-FDTD), which is an optimized high order variant of the nonstandard finite difference time domain method for electromaganetic wave propagation simulations (Cole, 1997, Balanis et al., 2009).

Our goal in this work is to improve the computation efficiency, reduce the modeling error at the specific targeted frequency significantly (~10 times lower), and provide an automatic method to derive the optimized coefficients for general cases. First, the conventional temporal finite difference approximation (3) is replaced by

$$\frac{\partial f^n}{\partial t} \approx \frac{f^{n+1/2} - f^{n-1/2}}{\frac{2}{\omega_0}\sin\left(\frac{\omega_0 \Delta t}{2}\right)}, \quad (4)$$

which is a better approximation of time derivative compared with the conventional finite difference scheme in terms of dispersion error. Furthermore, the error introduced by (4) will be further suppressed during the coefficient optimization to be discussed later.

The finite difference approximation of a spatial derivative (2) is written in a general form

$$\frac{\partial f_i}{\partial x} \approx \frac{c_{x1}(f_{i+1/2} - f_{i-1/2}) + c_{x2}(f_{i+3/2} - f_{i-3/2})}{\Delta x} \quad (5)$$

To optimize the coefficients for dispersion error reduction, we remove the constraint in (2)

$$c_{x1} + 3c_{x2} = 1. \quad (6)$$

The cost function representing the dispersion error at the specified frequency and propagation angle ranges is cast as:

$$C(c_{x1}, c_{x2}, c_{y1}, c_{y2}) = \frac{1}{2}\left\| F_{xi} + F_{yi} - F_0 \right\|^2 \quad (7)$$

$$F_{xi} = \left[c_{x1} \sin\left(\frac{\pi f \Delta x \cos\phi_i}{v} \frac{k^{num}}{k} \right) + c_{x2} \sin\left(\frac{3\pi f \Delta x \cos\phi_i}{v} \frac{k^{num}}{k} \right) \right]^2 \quad (8)$$

$$F_{yi} = \left(\frac{\Delta x}{\Delta y} \right)^2 \left[c_{y1} \sin\left(\frac{\pi f \Delta y \sin\phi_i}{v} \frac{k^{num}}{k} \right) + c_{y2} \sin\left(\frac{3\pi f \Delta y \sin\phi_i}{v} \frac{k^{num}}{k} \right) \right]^2 \quad (9)$$

$$F_0 = \left(\frac{\Delta x}{v \Delta t} \right)^2 \sin^2\left(\frac{\omega \Delta t}{2} \right) \quad (10)$$

Newton's method is employed to minimize the cost function (7), whose gradient $\mathbf{g}$ and Hessian matrix $\mathbf{H}$ are

$$\mathbf{g}_\xi = \frac{\partial C}{\partial \xi} = \sum_i \left(\frac{\partial F_i}{\partial c_\xi} \cdot F_i \right) \quad (11)$$

$$\mathbf{H}_{\xi_1 \xi_2} = \frac{\partial C}{\partial \xi_1 \partial \xi_2} \quad (12)$$

where $\xi \in \{c_{x1}, c_{x2}, c_{y1}, c_{y2}\}$.

The coefficients $c_{x1}, c_{x2}, c_{y1}, c_{y2}$ are obtained by solving

$$\Delta\boldsymbol{\xi}^n = -\mathbf{H}\mathbf{g}^n \quad (13)$$

$$\boldsymbol{\xi}^{n+1} = \boldsymbol{\xi}^n + \gamma^n \Delta\boldsymbol{\xi}^n, \quad (14)$$

where γ^n is the step length at n^{th} iteration .

With the derived coefficients in (14), we are able to update the wavefields using (4) and (5) to propagate seismic waves accurately (the accuracy performance will be shown in the numerical example section) and efficiently (note we only use 4-point stencil). The above nonlinear inversion process needs to be repeated for all the seismic wave velocity values. However, the computational cost is still negligible in comparison with wave propagation modeling itself. A less expensive strategy is conducting the coefficient optimization for several seismic individual velocities and then applying interpolation to obtain all the coefficients needed for wave propagation modeling.

Time-to-Frequency Domain Conversion

After the wave propagation simulation arrives at a steady state, time-to-frequency domain conversion is implemented during the simulation to output the frequency domain data. The time-to-frequency domain conversion technique was inspired by powerline harmonic removal methods based on orthogonality property of sinusoidal functions (Butler and Russell, 1993). In powerline harmonic removal problem, the signals are buried in the powerline harmonic noise.

$$M(t) = s(t) + \sum_{n=1}^{\infty} \left(a_n \cos n\omega_0 t + b_n \sin n\omega_0 t \right) \quad (15)$$

where $M(t)$ is the recorded data, $s(t)$ is the signal, and the second term on the right-hand-side is the harmonic noises. The phases and amplitudes of the harmonic noises can be estimated by

$$a_n = \frac{A_n \otimes M}{A_n \otimes A_n}, b_n = \frac{B_n \otimes M}{B_n \otimes B_n} \qquad t \to \infty , \tag{16}$$

where $A_n=cos(n\omega_0 t)$, $B_n=sin(n\omega_0 t)$, and $\otimes$ denotes cross correlation.

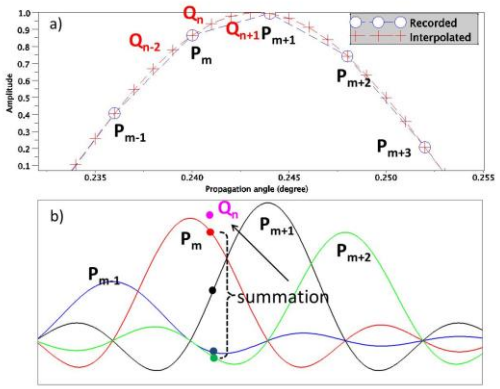

Figure 1: a) recorded values P and interpolated values Q for numerical integration; b) diagram for interpolation based on FIR filter design.

Our problem is actually easier to solve because there is no wide band signal in presence and the exact frequency is known. We only need to apply (16) on a segment (the segment length equals to one period or multiple periods) of the steady state simulation results. As a more general case, if a function $g(x)$ with orthogonal basis function $f(x)$ is defined on (a,b),

$$g = \sum_{i=1}^{n} c_i f_i \tag{17}$$

then we have

$$c_i = \frac{\int_a^b g(x) f_i(x) dx}{\int_a^b f_i^2(x) dx} \tag{18}$$

In our application, $f_1(x)=sin(x)$ or $f_2(x)=cos(x)$.

Although the discretization error introduced in finite difference simulation has been compensated as discussed earlier, the numerical integration error during the evaluation of (18) is still there if Δt is not small enough. As shown in Figure 1(a), if we only use recorded values P_i for the numerical integration in (18), the error will obviously introduced. Therefore, we need the interpolated values Q_i. To obtain error-free interpolation results for band-limited signal, ideally we should use infinite impulse response filter (IIR), which means we have to evaluate the contributions from all P_i. This is impractical because we cannot afford storing all the history variables. Instead, we design an FIR filter with window width specified by r (here we use $r = 2$), i.e.,

$$h[n] = h_d[n] w[n] \tag{19}$$

$$h_d[n] = \frac{\sin[\omega_c (n - n_d)]}{\pi (n - n_d)} \tag{20}$$

$$Q_n = \sum_{i=m-1}^{m+2} P_i h[(t_n - t_i)/\Delta t] \tag{21}$$

where ω_c is the cutoff frequency determined by Δt.

$w[n]$ is the window function, which can be designed through inversion by minimizing the following cost function

$$\max_{0 \le \delta n \le 0.5} \left| \sum_{n=-r}^{r} w[n+\delta n] h_d[n+\delta n] \exp[i\omega(n+\delta n)] - 1 \right| + \left| \sum_{n=-r}^{r} w[n+\delta n] h_d[n+\delta n] \exp[-i\omega(n+\delta n)] - 1 \right| \tag{22}$$

With (19)-(22), all the Q values can be obtained by using the neighboring four recorded P values. As shown in Figure 1(b), the interpolated Q_n value is the summation of the four weighted sinc functions at the specific location. These Q values are utilized in evaluating (18) to eliminate the time-to-frequency conversion error imposed by temporal discretization.

Numerical Analysis and Experiments

First, we conducted dispersion analysis of the conventional finite difference method and the optimized new scheme finite difference method (ONS-FD). Then, we ran numerical simulations to compare the performance of these two methods. Figure 2 shows the dispersion analysis result (numerical seismic velocity) as a function of propagation angle of 8th, 16th order conventional finite difference, and the new method. In this numerical example, Δt=2 ms,

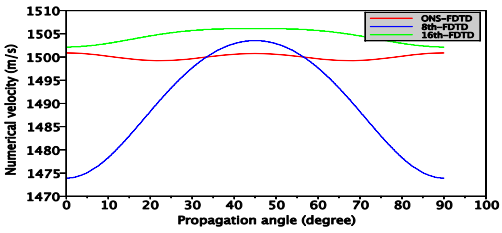

Figure 2: Dispersion relation for 8th order (blue), 16th order (green) conventional finite difference and ONS-FD (red), where Δt=2 ms, $\Delta x=\Delta z$=20 m, f=25 Hz, v_p=1500 m/s (i.e., PPW = 3).

Δx=Δz=20 m, f=25 Hz, v_p=1500 m/s (i.e., 3 points per wavelength). According to Figure 2, when φ=0 or φ=90° (horizontal or vertical propagation direction), 8th order FD has an error as large as 26 m/s; the error of ONS-FD is slightly lower than 16th order FD. When φ=45°, the error of 16th FD is much larger than ONS-FD. Interestingly, at this propagation direction, 16th order FD performs even worse than 8th order FD, which is confirmed by the simulation results shown in Figure 3(b). For all the propagation directions, the error of ONS-FD is controlled within ±1 m/s. The numerical simulation results plotted in Figure 3(a) and Figure 3(b) are consistent with the dispersion analysis, as expected.

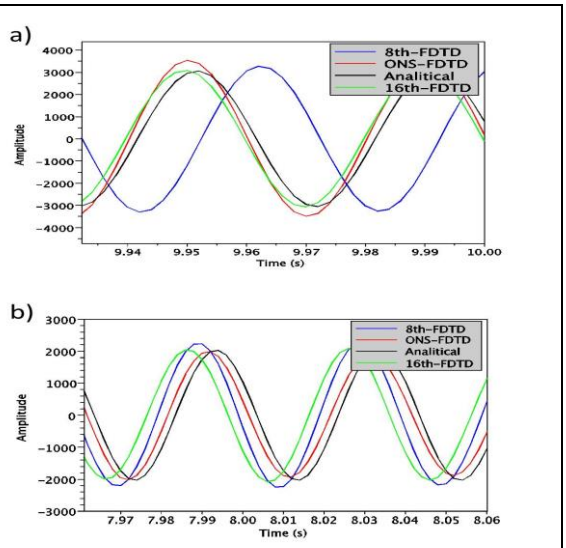

Figure 3: analytical solution (black) and numerical simulation results for 8th order FD (blue), 16th order FD (green), and ONS-FD (red), where Δt=2 ms, Δx=Δz=20 m, f=25 Hz, v_p=1500 m/s. a) propagation angle φ=0°; b) propagation angle φ=45°.

In the second numerical experiments, the horizontal grid size is different from the vertical grid size (a commonly used strategy in exploration geophysical applications). Δt=2 ms, Δx=20 m, Δz=10 m, f=25 Hz, v_p=1500 m/s (i.e., minimum point per wavelength is 3). Figure 4 shows the dispersion analysis results, where the ONS-FD shows excellent performance with the numerical velocity error suppressed below 0.3 m/s for all propagation angles. On the other hand, the error of 8th order FD varies with propagation angle from -28 m/s to +7 m/s while the error of the 16th order FD is more uniformly distributed over propagation angle (+2 m/s to +7 m/s). Again, the numerical simulation results in Figure 5(a) to Figure 5(c) are fully consistent with the dispersion analysis results in Figure 4.

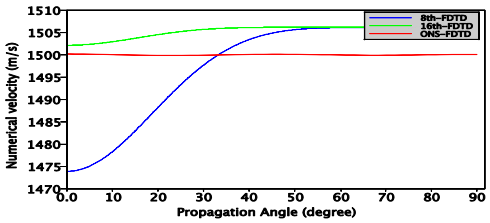

Figure 4: Dispersion relation for 8th order (blue), 16th order (green) conventional finite difference and ONS-FD (red), where Δt=2 ms, Δx=20 m, Δz=10 m, f=25 Hz, v_p=1500 m/s.

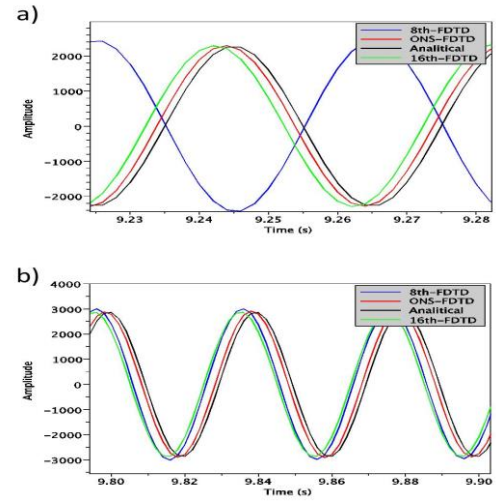

Figure 5: analytical solution (black) and numerical simulation results for 8th order FD (blue), 16th order FD (green), and ONS-FD (red), where , Δt=2 ms, Δx=20 m, Δz=10 m, f=25 Hz, v_p=1500 m/s. a) propagation angle φ=0°; b) propagation angle φ=90°.

Conclusions

An efficient and nearly exact seismic wave propagation modeling algorithm has been developed to be used as the engine of frequency domain full waveform inversion. With the combination of nonlinear inversion and FIR filter design technique, this new forward modeling algorithm is able to provide more accurate solutions than the 16th order conventional finite difference method at the similar computational expense as 4th order scheme. Another advantage of this method is that the numerical error is independent of time step size. In addition, numerical anisotropy, which is an inherent characteristic of the conventional finite difference method, has been eliminated effectively. The reason that this algorithm can be highly efficient and extremely accurate is that frequency domain FWI only deals with single frequency or narrow-band data.

References

Balanis, C. A., B. Yang, and C. R. Birtcher, 2009, Nonstandard and Higher-Order Finite-Difference Methods for Electromagnetics: ARIZONA STATE UNIV TEMPE DEPT OF ELECTRICAL ENGINEERING.

Bunks, C., F. M. Saleck, S. Zaleski, and G. Chavent, 1995, Multiscale seismic waveform inversion: Geophysics, 60, 1457–1473.

Butler, K. and R. Russell, 1993, Subtraction of powerline harmonics from geophysical records, Geophysics, 58(6), 898–903, doi: 10.1190/1.1443474

Cole, J.B., 1997, A high-accuracy realization of the Yee algorithm using non-standard finite differences, IEEE Transactions on Microwave Theory and Techniques,45(6), 991-996, doi: 10.1109/22.588615.

Plessix, R., 2009, Three-dimensional frequency-domain full-waveform inversion with an iterative solver: Geophysics, 74(6), WCC149–WCC157. doi: 10.1190/1.3211198

Pratt, R. G., C. Shin, and G. J. Hicks, 1998, Gauss-Newton and full Newton methods in frequency-space seismic waveform inversion: Geophysical Journal International, 13, 341–362.

Sirgue, L., and R. G. Pratt, 2004, Efficient waveform inversion and imaging: A strategy for selecting temporal frequencies: Geophysics, **69**, 231–248.

Tarantola, A., 1986, Astrategy for nonlinear elastic inversion of seismic reflectiondata: Geophysics, **51**, 1893–1903.

Vigh, D. and E. Starr, 2008, Comparisons for waveform inversion, time domain or frequency domain?. SEG Technical Program Expanded Abstracts 2008, 1890-1894. doi: 10.1190/1.3059269.

Vigh, D., B. Starr, J. Kapoor, and H. Li, 2010, 3D Full waveform inversion on a Gulf of Mexico WAZ data set: SEG Technical Program Expanded Abstracts 2010, 957-961. doi: 10.1190/1.3513935.